Separation Science and Technology
Publication details, including instructions for authors and subscription information:
http://www.informaworld.com/smpp/title~content=t713708471

Surface Force-Pore Flow Model in Predicting Separation and Concentration of Polyhydric Alcohols in Aqueous Solutions Using Cellulose Acetate Membranes

Bao Shiyao[a]; F. D. F. Talbot[a]; T. D. Nguyen[b]; T. Matsuura[b]; S. Sourirajan[b]
[a] DEPARTMENT OF CHEMICAL ENGINEERING, UNIVERSITY OF OTTAWA, OTTAWA, CANADA
[b] DIVISION OF CHEMISTRY NATIONAL RESEARCH COUNCIL OF CANADA, OTTAWA, CANADA

To cite this Article Shiyao, Bao , Talbot, F. D. F. , Nguyen, T. D. , Matsuura, T. and Sourirajan, S.(1988) 'Surface Force-Pore Flow Model in Predicting Separation and Concentration of Polyhydric Alcohols in Aqueous Solutions Using Cellulose Acetate Membranes', Separation Science and Technology, 23: 1, 77 — 90

To link to this Article: DOI: 10.1080/01496398808057635

URL: http://dx.doi.org/10.1080/01496398808057635

SEPARATION SCIENCE AND TECHNOLOGY, **23**(1-3), pp. 77-90, 1988

Surface Force-Pore Flow Model in Predicting Separation and Concentration of Polyhydric Alcohols in Aqueous Solutions Using Cellulose Acetate Membranes

---

BAO SHIYAO and F. D. F. TALBOT

DEPARTMENT OF CHEMICAL ENGINEERING
UNIVERSITY OF OTTAWA
OTTAWA, CANADA K1N 6N5

T. D. NGUYEN, T. MATSUURA, and S. SOURIRAJAN

DIVISION OF CHEMISTRY
NATIONAL RESEARCH COUNCIL OF CANADA
OTTAWA, CANADA K1A 0R6

Abstract

The reverse osmosis separation and concentration of polyhydric alcohols were experimentally tested by using cellulose acetate membranes of different average pore sizes. An attempt was made to predict membrane performance data, such as the solute separation and the product permeation rate, on the basis of the surface force-pore flow model, and the results were tested by experimental values. The processing capacities of the membranes were also calculated.

INTRODUCTION

The reverse osmosis (RO) separation, concentration, and fractionation of organic solutes in aqueous solutions are of practical interest as effective separation methods in the chemical, pharmaceutical, and food processing industries. Detailed studies on RO separations of ethylene glycol and propylene glycol (*1*) as well as monohydric and polyhydric alcohols (*2*) at various levels of solute concentration have been conducted and the results reported. The separation and the concentration of polyhydric alcohols, particularly of D-sorbitol, are of importance in terms of the production of the latter compound by hydrolysis of cellulose and subsequent hydrogenation for use in the pharmaceutical industry.

In order to analyze the above experimental data, Kimura-Sourirajan analysis has been applied, where the solute transport parameter of the solutes involved was correlated to their Taft numbers (*2*, *3*). These correlations offer a means for predicting the membrane performance for alcoholic solutes–water–cellulose acetate systems.

Recently, a transport model called the surface force-pore flow model (SFPF) (*4*) was reported as a quantitative expression of the preferential sorption-capillary flow mechanism (PSCF). The former model (SFPF) proved effective for the prediction of solute separation and membrane permeation data for a wide variety of solute–water systems. The SFPF model is particularly applicable for cases where either the solvent water or the solute is preferentially sorbed at the membrane solution interface, while Kimura-Sourirajan analysis is applicable to the case where the solvent is preferentially sorbed or the solutes are only weakly preferentially sorbed. The object of this paper is to collect more comprehensive experimental data for RO separations of polyhydric alcohols involving from two to six hydroxyl groups in the molecule from their aqueous solutions, to test the predictability of the SFPF model, and to calculate the processing capacity of cellulose acetate membranes for the RO separation of the above systems. Both calculated and experimental data are reported.

EXPERIMENTAL

Chromatography Experiments

The liquid chromatography model ALC 202 of Waters Associates fitted with a differential refractometer was used in this work. The method of column preparation and the general experimental technique were the same as those reported earlier (*5*). Briefly, solutes were injected into the solvent water stream which flows through a column packed with membrane polymer powder. The particle size was kept in the range 38–54 μm by sieving, and the column length was 60 cm. Ten microliters of sample solution (1 wt% solute) was injected into the column, and the retention volume was determined. In the case of heavy water, a 10 wt% solution was used as the sample. From the experimental retention volume data of solute A, $[V'_R]_A$, and of heavy water, $[V'_R]_{\text{water}}$, the specific surface excess $\Gamma_A/c_{A,b}$ of the solute was calculated as

$$\frac{\Gamma_A}{c_{A,b}} = \frac{[V'_R]_A - [V'_R]_{\text{water}}}{A_p} \tag{1}$$

where A_p denotes the total surface area of the polymer membrane material in the chromatography column.

RO Membranes

The membranes used in this study were produced according to the method described by Pageau and Sourirajan (*6*). The film casting composition was cellulose acetate (CA-398 supplied from Eastman Chemicals) 17 wt%, magnesium perchlorate 1.5 wt%, acetone 69.2 wt%, and water 12.3 wt%. The solvent was evaporated at 23°C for 1 min from the cast polymer solution of 4°C. After solvent evaporation the membrane was immersed in ice-cold water for gelation for more than 1 h. The membranes were then shrunk at different temperatures (60–89°C) to obtain different average pore sizes and pore size distributions.

RO Experiments

The apparatus and the experimental procedure used were the same as those reported by Kunst et al. (*7*). Each membrane was subjected to an initial pure water pressure of 8270 kPa gauge (= 1200 psig) for 3 h with pure water as feed to minimize the compaction effect. The specifications of all membranes are given in Table 1 in terms of pure-water permeability constant A (in kmol of $H_2O/m^2 \cdot s \cdot kPa$) and solute transport parameter, $D_{AM}/K\delta$, for sodium chloride (m/s) at 6890 kPag (= 1000 psig) with 3500 ppm NaCl–H_2O feed solution at feed flow rates corresponding to the mass transfer coefficient of 22×10^{-6} m/s on the high pressure side of the membrane. These were determined by Kimura-Sourirajan analysis (*8*). All other RO experiments were carried out at an operating pressure of 6890 kPag at a feed concentration of 100 ppm unless otherwise stated. In each experiment the fraction of solute separation, f, is defined as

$$f = \frac{\text{ppm in feed solution} - \text{ppm in product solution}}{\text{ppm in feed solution}}$$

TABLE 1
Specification of Reverse Osmosis Membranes Used[a]

Membranes[b]	$A \times 10^7$ (kmol H_2O)/ $m^2 \cdot s \cdot kPa$	$(D_{AM}/K\delta)_{NaCl}$ $\times 10^7$ m/s	Sodium chloride separation (%)	Product rate $\times 10^3$ kg/h
CA-unshrunk	19.58	273.0	44.1	112.0
CA-60	11.45	104.5	57.7	65.3
CA-70	7.69	6.33	89.7	42.2
CA-75	4.59	4.45	89.9	25.4
CA-80	3.09	1.10	93.9	16.6
CA-89	2.75	0.29	98.6	15.0

[a] Operating pressure, 6890 kPag (= 1000 psig); feed NaCl concentration, 0.06 m; $k = 22 \times 10^{-6}$ m/s.

[b] The numbers indicate the shrinkage temperatures.

and the product rate (PR) and the pure water permeation rate (PWP) in kg/h for given area of film surface, 13.2 cm^2 in this work, were determined under the specified experimental conditions. The data on PR and PWP were corrected at 25°C. Concentrations of NaCl were determined by conductance measurement, while concentrations of organic solutes were determined by a Beckman Total Carbon Analyzer Model 915-A.

THEORETICAL

Determination of Interfacial Interaction Force Constants

The transport equations based on the surface force-pore flow model, the procedure for the calculation of solute separations, pure water permeation rate, and product rate, which are obtainable by reverse osmosis experiments, the procedure for the determination of the interaction force constants from the liquid chromatography data, and the procedure for calculating the average pore size and the pore size distribution on the surface layer of asymmetric reverse osmosis membranes have been described elsewhere (*9–11*). For the clarification of symbols used in this paper, however, the framework of the theory is outlined below.

The solute separation f and the product rate PR can be calculated when data on PWP, pore size distribution, and interfacial interaction force constants are provided for given operating conditions of the experiment such as feed concentrations, operating pressure, and feed flow rate (*12*). The pore size distribution is expressed in terms of one or more Gaussian normal distributions. For describing such pore size distributions the distribution function of the *i*th distribution is given as

$$Y_i(R_b) = \frac{1}{\sigma_i\sqrt{2\pi}} \exp\left\{-\frac{(R_b - \bar{R}_{b,i})^2}{2\sigma_i^2}\right\} \tag{2}$$

and a quantity defined as

$$h_i = n_i/n_1 \tag{3}$$

are necessary, where $\bar{R}_{b,i}$, σ_i, and n_i denote the average pore size, standard deviation, and the number of pores which belong to the *i*th distribution (*12*). By definition, $\bar{R}_{b,i}$ becomes progressively larger as the number i increases.

With respect to nonionized organic solutes in aqueous solutions, the interfacial interaction force constants are expressed as constants which define the interfacial potential function by

$$\phi(d) = \begin{cases} \text{very large} & \text{when } d \leqslant \mathbf{D} \\ -\dfrac{\mathbf{B}}{d^3}\mathbf{R}T & \text{when } d > \mathbf{D} \end{cases} \tag{4}$$

where d is the distance between the polymer surface and the center of the solute molecule, **D** is a constant associated with the steric hindrance (distance of steric repulsion), and **B** expresses the nature and the magnitude of the van der Waals force. The quantity **D** is always positive, and when the solute shape is assumed spherical, it can be approximated by the molecular radius such as the Stokes' law radius, while **B** may be either positive (corresponding to an attractive force) or negative (corresponding to a repulsive force). The parameters associated with the pore size distribution, i.e., $\bar{R}_{b,i}$, σ_i, and h_i, and the interfacial interaction force parameters **B** and **D** are related to specific surface excess $\Gamma_A/c_{A,b}$, obtainable from the chromatographic experiment, and the solute separation f, obtainable from RO experiments by the following equations:

$$(\Gamma_A/c_{A,b})_j = \{g(\mathbf{B},\mathbf{D})\}_j \tag{5}$$

$$f_j = \{h(\bar{R}_{b,i},\sigma_i,h_i,\mathbf{B},\mathbf{D};\ \text{under given operating conditions}\}_j \tag{6}$$

where subscript j indicates the jth solute, and $g(\dots)$ and $h(\dots)$ are some functional forms established in the SFPF model (*4*, *10*). Using the above equations, the numerical values for the pore size distribution parameters and the interfacial interaction force parameters can be determined as follows.

Cases in Which a Uniform Pore Size Distribution Is Involved

1) Determination of **B** and **D** values for a reference solute. Only one reference solute is considered; therefore $j = 1$. For this solute, **D** is approximated by the Stokes' law radius of the solute. The numerical value of **B** can then be obtained from Eq. (5) using experimental values of $\Gamma_A/c_{A,b}$ for the reference solute.

2) Determination of the average pore radius $\bar{R}_{b,1}$. Only a uniform pore of $\bar{R}_{b,1}$ is considered. $\bar{R}_{b,i>1}$, σ_i, and h_i can be considered to be equal to zero. Since we know **B** and **D** values from Step 1, $\bar{R}_{b,1}$ can be immediately calculated from Eq. (6) by using experimental data of f_1 for the reference solute.

3) Determination of **B** and **D** values for solutes other than the reference solute. Once $\bar{R}_{b,1}$ is known, **B** and **D** values for the solutes other than the reference solute can be obtained by simultaneous solutions of Eqs. (5) and (6) for each solute such that experimental $\Gamma_A/c_{A,b}$ and f data can be satisfied.

Cases in Which Two Normal Pore Size Distributions Are Considered

In two normal distributions, five parameters, namely $\bar{R}_{b,1}$, σ_1, $\bar{R}_{b,2}$, σ_2, and h_2, are necessary in order to characterize the pore size distribution on the membrane surface. Five or more reference solutes are necessary for obtaining such parameters. In this paper we have used seven reference solutes. Setting Eqs. (5) and (6) for each reference solute, we have seven Eq. (5) and seven Eq. (6), corresponding to $j = 1, 2, 3, \dots, 7$.

4) Determination of **B** and **D** values for reference solutes. Again, setting $(\mathbf{D})_j$ equal to the Stokes' law radius of the jth reference solute, $(\mathbf{B})_j$ can be calculated from Eq. (5) established for the jth solute, so that experimental $(\Gamma_A/c_{A,b})_j$ can be satisfied.

5) The five pore size distribution parameters mentioned above can be calculated by nonlinear regression analysis of seven Eq. (6)'s by using **B** and **D** values obtained above for each reference solute.

Calculation of Solute Separation and Product Rate

Once the pore size distribution parameters $\bar{R}_{b,1}$, σ_1, $\bar{R}_{b,2}$, σ_2, and h_2 are known for a membrane, and the interfacial interaction force parameters **B** and **D** are known for a given system of membrane material-solute, solute separation f can be calculated by Eq. (6) for any combination of the above parameters. Furthermore, since the PR/PWP ratio can also be calculated by the surface force-pore flow model (*4*), PR is obtained by multiplying experimental PWP data by the above ratio.

Calculation of Processing Capacities

The processing capacity of a membrane $(V)_i/St$, m^3/m$^2 \cdot$ d, is defined as the volume of charge (feed solutions) that 1 m^2 of film surface can handle per day in a batch concentration process to increase the solute weight fraction from $(z)_i$ to $(z)_f$ at a given operating pressure. The following relationship has been derived by Sourirajan and Kimura (*13*):

$$\frac{(V)_i}{St} = \left[(\rho_l)_i \int_{(z)_i}^{(z)_f} \frac{\exp\left\{ \int_{(z)_i}^{z} \frac{dz}{z-a} \right\}}{G(z-a)} dz \right]^{-1} \tag{7}$$

where z and a denote weight fractions (ppm) of solute in the solution at the high pressure side of the membrane and product, respectively, and ρ_l and G are the density of the solution, kg/m^3, and product permeation flux, kg/m$^2 \cdot$ d, respectively. Subscripts i and f represent, respectively, the initial and final states of the given feed solutions on the high pressure side of the membrane. Equation (7) allows the calculation of the processing capacity by performing the numerical integration of the right side of the equation from $z = (z)_i$ to $z = (z)_f$ since G (product permeation flux) versus z (ppm of the feed solution) data as well as a (ppm of product solution) versus z become available from the foregoing calculations. As is obvious from Eq. (7), the processing capacity $(V)_i/St$ can be given as a function of $(z)_f/(z)_i$.

RESULTS AND DISCUSSION

Determination of B and D Values

A compilation of the data on **B** and **D** values for a large number of organic solutes has been made by Sourirajan (*14*). In the process of generating such values, glycerol was chosen as the reference solute in the Step 1 calculation. The average pore size on the membrane surface was then determined for a membrane by the Step 2 calculation. Using the pore size determined above, **B** and **D** values were calculated by Step 3 for solutes other than the reference solute. **B** and **D** values for 1,2-ethanediol, glycerol, xylitol, and D-sorbitol are from Sourirajan's table (*14*). Those values for erithritol were newly generated in this work by the same procedure as above. All the data for different polyhydric alcohols so obtained are listed in Table 2 with respect to cellulose acetate E-398 material. It should be noted that **B** values of the above solutes are negative without exception, indicating the rejective force exerted on the solute by the membrane material. Furthermore, **B** values become progressively more negative as the solute size increases.

Determination of the Pore Size Distribution on the Surface of Cellulose Acetate Membranes Used

A series of crown ethers with molecular weights ranging from 58 to 264, listed in Table 2, have been chosen as reference solutes, whose **B** and **D** values obtained from Step 4 with respect to the CA-398–water system are

TABLE 2

Interfacial Interaction Force Parameters for Reference Solutes and Polyhydric Alcohols

Solutes	Molecular weight	$\mathbf{D} \times 10^{10}$ m	$\mathbf{B} \times 10^{30}$ m^3
Reference solutes:			
1,3-Dioxolane	74.1	1.96[a]	42.43[a]
Trimethylene oxide	58.1	2.06	34.60
p-Dioxane	88.1	2.23[a]	53.87[a]
Tetrahydropyran	86	2.38	48.03
12-Crown-4	176.2	3.19[a]	28.68[a]
15-Crown-5	220.3	3.77[a]	−321.80[a]
18-Crown-6	264.3	4.29[a]	−202.60[a]
Polyhydric alcohols:			
1,2-Ethanediol	62	2.20[b]	−16.82[b]
Glycerol	92	2.30[b]	−52.30[b]
Erithritol	122	2.94	−96.10
Xylitol	152	3.30[b]	−135.00[b]
D-Arabitol	182	4.64[b]	−180.20[b]

[a] Data reproduced from Nguyen et al. (*15*).

[b] Data reproduced from Sourirajan (*14*).

also listed in Table 2. **B** and **D** values for 1,3-dioxolane, *p*-dioxane, 12-crown-4, 15-crown-5, and 18-crown-6 are reproduced from the literature (*15*), while those for trimethylene oxide and tetrahydropyran were newly obtained in this work. By using the above **B** and **D** values, the average pore size and the pore size distribution on the surface of membranes shrunk at different temperatures were calculated following Step 5. The results, shown in Table 3, indicate that all membranes other than CA-89 membrane possess two pore size distributions, one with average radii in the range from 7.7 to 9.6×10^{-10} m and the other from 42 to 58×10^{-10} m. Both $\bar{R}_{b,1}$ and $\bar{R}_{b,2}$ decrease with an increase in the shrinkage temperature. In the case of CA-89 membranes, however, h_2 is equal to zero, indicating the disappearance of the second pore of larger radii. In Table 4 the experimental separation data of reference solutes are compared with those data calculated on the pore size distribution reported in Table 3. The satisfactory agreement testifies to the validity of the transport model used, the interaction force parameters, and the pore size distributions.

Predictability of Solute Separation and Membrane Permeation Rate by SFPF Model

The interfacial force parameters **B** and **D** for polyhydric alcohols listed in Table 2 and the pore size distribution data listed in Table 3 were then combined to calculate solute separations of different polyhydric alcohols from dilute aqueous solutions by membranes of different pore size distributions. The results shown in Table 5 indicate there is excellent agreement between experimental and calculated values within an error range of ±3%. It should be noted that the above comparison is a true test

TABLE 3

Average Pore Size and Pore Size Distribution of Cellulose Acetate Membranes Shrunk at Different Temperatures

Membranes[a]	$\bar{R}_{b,1} \times 10^{10}$ m	$\sigma_1/\bar{R}_{b,1}$	$\bar{R}_{b,2} \times 10^{10}$ m	$\sigma_2/\bar{R}_{b,2}$	h_2
CA-unshrunk	9.6	0.20	58	0.40	0.003
CA-60	8.9	0.32	53	0.45	0.003
CA-70	8.6	0.001	40	0.001	0.001
CA-75	8.8	0.001	47	0.001	0.001
CA-80	8.5	0.001	42	0.001	0.001
CA-85	7.7	0.001	—	—	0

[a] The numbers indicate the shrinkage temperatures.

TABLE 4
Comparison of Experimental and Calculated Separation Data of Reference Solutes[a]

		Solute separation (%)[c]						
Membranes	PWP × 10^3 kg/h[b]	1,3-Dioxolane	Trimethylene oxide	*p*-Dioxane	Tetrahydropyran	12-Crown-4	15-Crown-5	18-Crown-6
CA-unshrunk	111.7	1.9	6.6	—	17.0	39.1	—	64.3
		(1.4)	(4.0)	—	(18.0)	(43.7)	—	(62.1)
CA-60	56.2	3.8	—	8.3	6.7	62.4	—	82.9
		(0.0)	—	(4.7)	(11.5)	(60.0)	—	(81.2)
CA-70	38.5	8.2	16.7	30.0	—	91.0	93.6	95.7
		(6.1)	(19.0)	(31.0)	—	(88.2)	(95.6)	(96.0)
CA-75	22.5	9.5	15.8	29.2	—	91.0	94.9	98.5
		(8.3)	(15.8)	(31.8)	—	(89.2)	(95.4)	(95.4)
CA-80	15.6	14.2	21.7	—	50.0	91.0	96.2	97.1
		(10.0)	(26.0)	—	(55.6)	(91.2)	(96.6)	(96.4)
CA-89	15.9	28.0	39.4	—	65.8	97.0	99.8	99.8
		(27.0)	(42.7)	—	(65.7)	(96.1)	(99.9)	(99.9)

[a] Solute concentration in feed, 100 ppm; operating pressure, 6890 kPag (= 1000 psig); PR ≃ PWP; feed flow rate, corresponding to $k_{NaCl} = 22 \times 10^{-6}$ m/s.

[b] Membrane area = 13.2 cm^2.

[c] Experimental values without parentheses; calculated values in parentheses.

TABLE 5
Comparison of Experimental and Predicted Solute Separation for Different Polyhydric Alcohols[a]

Membranes	PWP × 10^3 kg/h[b]	Solute separation (%)[c]				
		1,2-Ethanediol	Glycerol	Erithritol	Xylitol	D-Sorbitol
CA-unshrunk	106.7	17.5	26.6	—	58.7	66.1
		(14.3)	(23.4)	(51.4)	(60.5)	(66.3)
CA-60	52.4	30.2	39.4	62.9	75.2	83.1
		(25.6)	(38.1)	(66.5)	(75.6)	(82.0)
CA-70	36.5	62.7	76.1	90.3	93.4	94.9
		(62.0)	(77.9)	(92.8)	(94.7)	(95.9)
CA-75	20.2	58.7	72.5	88.7	91.7	94.9
		(61.7)	(78.1)	(92.9)	(94.6)	(95.7)
CA-80	13.8	—	85.3	93.5	95.0	96.6
		(69.7)	(83.2)	(94.5)	(95.8)	(96.7)
CA-89	15.0	85.7	90.8	96.8	98.3	100
		(82.8)	(91.9)	(98.6)	(99.3)	(99.9)

[a] Operating pressure, 6890 kPag (= 1000 psig); feed solute concentration, 100 ppm; PR ≈ PWP; feed flow rate, corresponding to $k_{NaCl} = 22 \times 10^{-6}$ m/s.

[b] Film area = 13.2 cm^2.

[c] Experimental values without parentheses; predicted values in parentheses.

of the computation model and the associated parameters since the membrane from which interfacial force parameters for polyhydric alcohols were generated is not included in the membranes by which the testing was performed. Another test was the separation and product rate data of D-sorbitol at concentration changing from 100 ppm to 15 wt%. Membranes CA-70, CA-75, CA-80, and CA-89 were used in the experiments. As the results shown in Table 6 indicate, there is excellent agreement between the experimental values and those calculated on the basis of the SFPF model.

Processing Capacity

By using the data on solute separation and membrane permeation rate obtained in the foregoing section, the processing capacities of membranes for a 1 wt% aqueous D-sorbitol solution at 6890 kPag were calculated with respect to CA-70 and CA-89 films. The results are shown in Fig. 1. The volumes which can be handled by 1 m^2 of the membrane in 1 d are 0.54 and 0.24 m^3 for CA-70 and CA-89 films, respectively, when 1

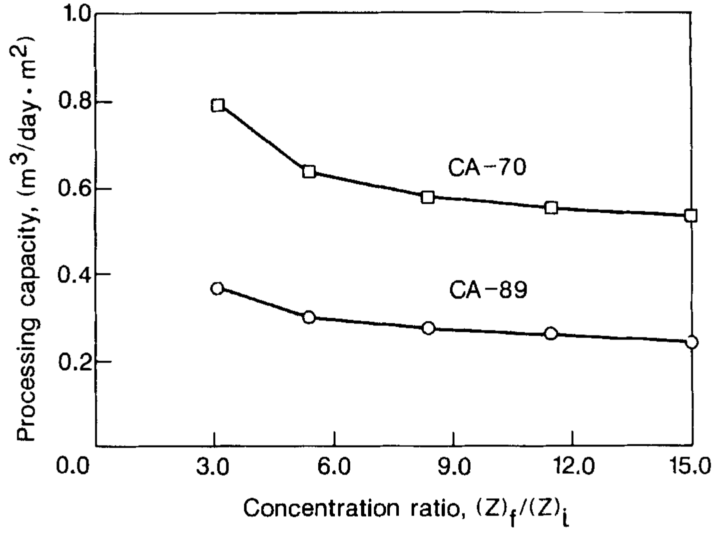

FIG. 1. Processing capacities of membranes for the concentration of 1 wt% aqueous D-sorbitol solution at an operating pressure of 6890 kPa gauge (= 1000 psig). Membrane material: cellulose acetate.

TABLE 6

of Experimental and Predicted Reverse Osmosis Performance of D-Sorbitol in Aqueous Solution at Different Feed

Solute concentration in feed (ppm)^b										
100		30,500		53,400		83,400		114,400		
PR	*f*	PR	*f*	PR	*f*	PR	*f*	PR	*f*	PR
34.8	94.9	24.6	93.6	23.8	94.8	21.5	93.6	17.9	94.9	14
(34.8)	(95.9)	(25.2)	(96.4)	(23.1)	(96.3)	(20.7)	(96.2)	(19.5)	(96.2)	(18
19.8	94.9	16.5	94.9	15.2	94.8	13.9	93.6	11.9	94.8	9
(19.8)	(95.7)	(15.7)	(95.8)	(15.1)	(95.8)	(13.4)	(95.7)	(12.9)	(95.7)	(12
13.1	96.6	11.3	96.2	10.4	96.5	9.7	97.5	8.4	96.6	6
(13.1)	(96.7)	(11.3)	(96.7)	(10.7)	(96.7)	(9.5)	(96.7)	(9.1)	(96.6)	(8
14.6	100	13.1	100	12.1	100	10.8	100	9.3	100	7
(14.6)	(99.9)	(13.1)	(99.9)	(12.1)	(99.9)	(10.7)	(99.9)	(10.3)	(99.8)	(9

g pressure, 6890 kPag (= 1000 psig); feed flow rate, corresponding to $k_{NaCl} = 22 \times 10^{-6}$ m/s; film area = 13.2 cm^2.
ental values without parentheses; predicted values in parentheses; PR = product rate × 10^3 kg/h; *f* = solute separati

wt% D-sorbitol is concentrated to 15 wt% under the specified experimental conditions.

CONCLUSION

It is concluded that cellulose acetate membranes of small pore sizes are effective in the separation and concentration of polyhydric alcohols such as D-sorbitol. It has also been concluded that the surface force-capillary flow model and associated numerical parameters are useful for predicting membrane performance data such as solute separation and the product permeation rate. The processing capacities of cellulose acetate membranes used for the experiment were found to be 0.24 ~ 0.54 $m^3/d \cdot m^2$, depending on the pore size of the membrane, when 1 wt% of D-sorbitol is concentrated to 15 wt% at 6890 kPag (= 1000 psig).

Acknowledgments

The authors are grateful to T. A. Tweddle for his technical assistance. Issued as NRC No. 28569.

REFERENCES

1. T. Matsuura and S. Sourirajan, *Ind. Eng. Chem., Process Des. Dev., 10,* 102 (1971).
2. T. Matsuura and S. Sourirajan, *J. Appl. Polym. Sci., 17,* 1043 (1973).
3. T. Matsuura and S. Sourirajan, *Ibid., 15,* 2905 (1971).
4. S. Sourirajan and T. Matsuura, *Reverse Osmosis/Ultrafiltration Process Principles,* National Research Council of Canada, Ottawa, 1985, Chap. 4.
5. T. Matsuura, P. Blais, L. Pageau, and S. Sourirajan, *Ind. Eng. Chem., Process Des. Dev., 16,* 510 (1977).
6. L. Pageau and S. Sourirajan, *J. Appl. Polym. Sci., 16,* 3185 (1972).
7. B. Kunst and S. Sourirajan, *Ibid., 14,* 2559 (1970).
8. S. Sourirajan, *Reverse Osmosis,* Academic, New York, 1970, Chap. 3.
9. T. Matsuura and S. Sourirajan, *Ind. Eng. Chem., Process Des. Dev., 20,* 273 (1981).
10. T. Matsuura, Y. Taketani, and S. Sourirajan, in *Synthetic Membranes,* Vol. 2 (A. F. Turbak, ed.), ACS Symposium Series 154, American Chemical Society, Washington, D.C., 1981, p. 315.
11. K. Chan, T. Matsuura, and S. Sourirajan, *Ind. Eng. Chem., Prod. Res. Dev., 21,* 605 (1982).
12. K. Chan, T. Liu, T. Matsuura, and S. Sourirajan, *Ibid., 23,* 124 (1984).
13. Ref. *8,* Chap. 6.
14. S. Sourirajan, *Lectures on Reverse Osmosis,* National Research Council of Canada, Ottawa, 1983.
15. T. D. Nguyen, K. Chan, T. Matsuura, and S. Sourirajan, *Ind. Eng. Chem., Prod. Res. Dev., 23,* 501 (1984).

Received by editor January 21, 1987